

Renaissance for Low Shrinking Resins: *all-in-one* Solution by Bi-Functional Vinylcyclopropane-Amides**

*Paul Pined Contreras,^a Christian Kuttner,^b Andreas Fery,^b Ullrich Stahlschmidt,^c
Valérie Jérôme,^c Ruth Freitag,^c and Seema Agarwal^{a*}*

^{a.} *Macromolecular Chemistry II, Universität Bayreuth, Universitätsstrasse 30, 95440
Bayreuth, Germany, E-mail: agarwal@uni-bayreuth.de; Tel: +49-921-553397*

^{b.} *Physical Chemistry II, Universität Bayreuth, Universitätsstrasse 30, 95440 Bayreuth,
Germany*

^{c.} *Process Biotechnology, Universität Bayreuth, Universitätsstrasse 30, 95440 Bayreuth,
Germany*

Content

Materials.....	3
Methods	3
Monomer Synthesis.....	8
Synthesis of diethyl 2-vinylcyclopropane-1,1-dicarboxylate (1) and 1-(ethoxycarbonyl)-2-vinylcyclopropanecarboxylic acid (1a).....	8
Complexness of isomerization for VCP derivatives.....	8
Synthesis of 1,2-bis[(1-ethoxycarbonyl-2-vinylcyclopropan--1yl)carbonyloxy]hexane (VCPHexEster)	9
Synthesis of diethyl-1,1'-(2,4,4-trimethylhexane-1,6-diyl)bis(azanediyl)bis-(oxomethylene)bis(2-vinylcyclopropanecarboxylate) (VCPMe ₃ hexAmid).....	13
Supplementary Analytical Data	16
Temperature variable 1H-NMR experiment to confirm the hydrogen bonding effect of the VCP-amide resin (VCPMe ₃ hexAmid)	16
Photo-polymerization mechanism of bi-functional VCP derivatives	17
High resolution solid state ¹³ C-NMR spectroscopy of cured VCPMe ₃ hexAmid.....	18
Spectroscopic Ellipsometry: Refractive index measurements	19
Determination of mechanical properties (E-Modulus)	20
Determination of residual monomer amount of cross-linked samples by extraction experiments.....	20
Compilation of characteristic resin features	23
Determination of Cytotoxicity:.....	23
References.....	25

Materials

Trans-1,4-dibromo-2-butene (99 %), potassium hydroxide (KOH, >85 %), diethyl malonate (99 %), N,N'-dicyclohexylcarbodiimide (DCC, 99 %), 4-(dimethylamino)pyridine (DMAP, >98 %), 2,2,4(2,4,4)-trimethyl-1,6-hexandiamine (99 %), hexamethylenediamine (HMDA, 98 %), 1,6-hexandiol (99 %), triethylamine (99 %), ethyl 4-(dimethylamino)benzoate (EDMAB, 99 %), 1,3,5-trimethylbenzene (mesitylene, >99.8 %), camphorquinone (CQ, 97 %) and dichloromethane (>99.5 %) were supplied by Sigma Aldrich and used without further purification. 1-hydroxybenzotriazole (HOBt anhydrous) (Omnilab Life Science / OLS) and ethanol absolute (EtOH, >99 %) (VWR) were used as received. Sodium (cubes, delivered in mineral oil) (Aldrich, 99 %) was purified by melting in dry xylene prior to use. Urethane-dimethacrylate (UDMA), dodecanediol-dimethacrylate (1,12-DMA) and a 6:4 mixture of bisphenol-A-glycidyl methacrylate (BisGMA) and triethylene-glycol-dimethacrylate (TEGDMA) have been gratefully provided by the Kettenbach GmbH (Eschenburg, Germany) and were used as received.

Methods

Nuclear magnetic resonance (NMR) spectroscopy: Both ^1H - (300 MHz) and ^{13}C - (75 MHz) NMR spectra were recorded on a Bruker Ultrashield-300 spectrometer at 20 °C in CDCl_3 . The spectra were calibrated on the solvent signal ($\delta(^1\text{H}) = 7.26 \text{ ppm}$; $\delta(^{13}\text{C}) = 77.16 \text{ ppm}$). High-resolution solid state ^{13}C CP/MAS (cross polarization/magic angle spinning) NMR Spectra were measured by a Bruker spectrometer operating at 100.6 MHz, using a pulse experiment with a 30 s pulse delay for 2048 scans. The ^{13}C signals of the olefinic groups in uncured and cured VCPMe₃hexAmid resin are observed at about 133 and 119 ppm for the uncured and at about 129 ppm for the cured VCPMe₃hexAmid resin, respectively. In order to evaluate the spectra, MestReNova (Mestrelab Research, version 6.1) was used.

Gas chromatography (GC): GC measurements have been done by a GC-FID system (QP-5050) from Shimadzu company, using nitrogen as carrier gas. The injector temperature was 300 °C. The reaction mixtures were dissolved in acetone (2 $\mu\text{L mL}^{-1}$), 1 μL was injected in a split ratio of 1:50 and measured from 50 °C (2 min hold) up to 300 °C with a heating rate of 15 K min⁻¹. Software: LabSolutions (Shimadzu, version 5.54 SP2).

Gas chromatography-mass spectrometry (GC-MS):

GC-MS measurements were carried out on a Agilent system (5977A MSD), using helium as carrier gas. The injector temperature was 300 °C. The reaction mixtures were dissolved in acetone (2 $\mu\text{L mL}^{-1}$), 1 μL was injected in a split ratio of 1:50 and measured from 50 °C (2 min hold) up to Maestro 1 GCMSD/EnhancedMassHunter (Gerstel, version 1.4.23.11) (Shimadzu, version 5.54 SP2).

Medium Pressure Silica gel Chromatography (MPLC):

MPLC purifications were performed with a GRACE Reveleris X2 system operating with an integrated UV-VIS and ELSD detector for fraction detection. Commercial grade solvents were distilled before use.

Photo-Differential Scanning Calorimetry (Photo-DSC):

Photo-DSC measurements were carried out on a Perkin-Elmer Photo-DSC instrument (DSC 7) at isothermal conditions of 35 °C in a nitrogen atmosphere (flow rate = 50 mL/min) with 20 ± 5 mg of sample amount. Before irradiation, each sample has been purged with nitrogen for 4 minutes to avoid oxygen inhibition. The instrumental setup consists of a 450 W xenon lamp as light source, whose light beam was passed through an IR absorbing water filter and a grey filter to reduce the light total intensity to 10 %. An optical splitter was used to part the light beam into a sample and a reference beam, which were focused to the polymerizable samples and an empty reference pan respectively. The light intensity accounted to 6.93 mW cm^{-2} . The heat flow of polymerization reaction was recorded as a function of time. The polymerizable samples were prepared by dissolving the photo initiators in the respective monomer mixture in a brown glass vial at 25 °C in a shaking device for an appropriate time.

Dielectric Analysis (DEA):

Photo-curing experiments have been monitored by dielectric analysis on a DEA Epsilon 288 from NETZSCH company at 35 °C isothermal conditions, using IDEX 115/40 sensor types with frequencies of 1, 10, 100, and 1000 Hz and an OmniCure S2000 UV lamp as radiation source, whose light emission was filtered by an optical filter to a spectrum of 400-500 nm.

Spectroscopic Ellipsometry (SE): Refractive index measurements

SE was done in polarizer-compensator-sample-analyzer (PCSA) configuration (SE800, Sentech) with a xenon lamp as white-light source. The ellipsimetric ratio ρ was measured from 380 to

680 nm at angles of incidence of $\phi = 60^\circ$, 65° , and 70° at 3 different positions of the sample. Each incidence angle was evaluated using Eq. 1. After averaging over ϕ , the respective standard deviation was calculated from the Gaussian error propagation on basis of the variation of $\rho(\lambda, \phi)$. For a simple two-media interface, the complex optical properties of the bottom layer can be directly evaluated by the pseudo-dielectric function:^[1]

$$n_{\text{bottom}}^2 = n_{\text{top}}^2 \sin^2 \phi [1 + \tan^2 \phi (1 - \rho)^2 / (1 + \rho)^2] \quad \text{with} \quad \rho(\lambda, \phi) = r_p / r_s \quad \text{Eq. 1}$$

For light incident from an ambient medium n_{top} of known refractive index ($n_{\text{air}} = 1$), the optical properties of the reflecting bottom medium n_{bottom} can be determined directly from the measured ellipsometric ratio ρ and the angle of incidence ϕ . From the resulting wavelength-dependent dispersion, the refractive index at 589 nm was calculated. The change in refractive index Δn was calculated from the bulk index of polymer in reference to the monomer index.

Dynamic Mechanical Thermal Analysis (DMTA): E-Modulus determination

A dynamic-mechanical analyzer (DMTA IV) from Rheometric Scientific has been used to determine the E-moduli by three-point bending tests, using specimens of the dimension $25 \times 3 \times 1 \text{ mm}^3$. The experiments were conducted within the linear-elastic range, a span width of 20 mm, strain rates of 2 mm/min and at room temperature (20 °C with a relative humidity of 70 %). For the computer-based evaluation, equation (2) was used to calculate the E-modulus

$$E_{B3} = \frac{l_v * h * F_2 - F_1}{8 * J * 0,002} \text{N mm}^{-2} \quad \text{Eq. 2}$$

where F are the used forces (in N); l_v is the test span (in mm), J is the area moment of inertia, and h is the thickness of the respective specimen (in mm). The E-modulus was determined by the linear slope of the graphical analysis of the flexural stress against the sample strain.

Vickers Hardness:

A MHT-10 cap in combination with an optical microscope from Leica was used to perform Vickers hardness measurements in dependence of the used load. The loading time differs between 15-30 s. Five samples for each polymer with forces between 20-200 mN were used to define the Vickers hardness.

Rheometric Measurements:

Viscosity testing was carried out with a cone-plate rotation viscometer PK 100, coupled with a RV 20-M5 Rotavisco analyzer and a RC 20 controller from Haake. The viscosity has been

measured in dependence of the shearing rate at 25 ± 0.5 °C with ~ 0.5 mL of sample amount respectively. Rheowin software was used for acquisition. All values represent the average of five measurements and refer to a shearing rate of 100 s^{-1} .

Preparation of Polymer Networks:

To perform the monomer photo-activation a homemade photo reactor in the dimension $450 \times 450 \times 300 \text{ mm}^3$ including 22 Cree XM-L LEDs (dominant wavelength emission of blue-light LED 450-465 nm) was used as radiation source. The radiant flux of the photo reactor (scattered light) was determined to 2.013 mW cm^{-2} by a NEWPORT Multi-Function Optical Meter (1835-C) respectively for 465 nm. The preparation of the polymer specimens were carried out in dependence of the instrumental experiment. The specimens for the DMTA measurements were produced by filling a stainless steel profile with five equal milled edges with a dimension of $25 \times 3 \times 1 \text{ mm}^3$ with the current monomer/initiator mixture. The profile was enclosed and fixed both on top and on the bottom with a $100 \mu\text{m}$ thick Hostophan sheet. Finally, the profile was irradiated for 2 h within the photo reactor. The cured polymer was pressed out carefully and has been stored for 24 h at room temperature prior testing. To avoid measurement deviations cause of volume shrinkage the final specimen dimension of ca. $25 \times 3 \times 1 \text{ mm}^3$ was verified exactly by using a digital measuring slide. The specimens for the Vickers hardness measurements have been prepared by coating $400 \mu\text{m}$ thick monomer/initiator mixtures with a doctor knife on a glass slide. The glass slide has been infiltrated to a desiccator, flushed constantly with argon as protection gas. Finally, the desiccator has been irradiated for 2 h within the photo reactor. The homogenous and cured polymer samples were stored for 24 h at room temperature prior testing. The preparation of the specimens for the ellipsometric measurements occurred analog to the samples assigned for the Vickers hardness besides the samples were cured on silicon wafers.

Determination of Residual Monomer Amount:

While the quantification of the residual VCPHexEster monomer from the cured samples was performed by GC, the residual amount of the VCPMe₃hexAmid was performed by ^1H -NMR measurements, as this monomer was due to its higher molar mass and polarity within GC measurements not detectable. According to the VCPHexEster monomer conversion within the Photo-DSC experiments, the weighted and cured samples have been immediately immersed after radiation to 5.0 mL of chloroform (as extraction fluid) in 10 mL bottles with snap-on caps for 24 h respectively. The residual monomer amounts have been calculated by comparison the

integration areas of the samples with the previous established calibration curve. According to the VCPMe₃hexAmid monomer, the weighted and cured samples have been immediately immersed after radiation to 1.0 mL of CDCl₃ (as extraction fluid) in 2 mL bottles with snap-on caps for 24 h respectively. The residual monomer amounts have been calculated by comparison the integration areas of the respective ¹H-NMR proton signals (amide-, vinyl and cyclopropane-protons) to the proton signals of mesitylene, which has been added to the CDCl₃ as internal standard in 2.8216 mg mL⁻¹ amount. The concentration range of the previous established calibration curve of the VCPMe₃hexAmid amounted between 5 mg mL⁻¹ and 0.01 mg mL⁻¹. For each ¹H-NMR a number of scans of 2048 has been chosen to achieve an appropriate signal to noise resolution.

Determination of Volume Shrinkage:

The polymerization shrinkage was calculated from the difference in density of the monomer to the formed polymers by using Archimedes's principle. Applying a 1 mL pycnometer at room temperature the densities of the monomers were measured by taring the density. For the cured samples the densities have been calculated by its water displacement, respectively for ~400 mg cured specimens. The shrinkage of polymerization was determined separately for three samples and adjusted to the confirmed monomer conversion respectively.

Determination of Cytotoxicity:

The cytotoxicity of the VCPMe₃hexAmid, VCPHexEster and UDMA was tested using L929 murine fibroblasts (CCL-1, ATCC) according to the norm ISO 10993-5 using 1 mg mL⁻¹ MTT-stock solution. The L929 cells were maintained in MEM cell culture medium supplemented with 10 % fetal calf serum (FCS), 100 mg mL⁻¹ streptomycin, 100 IU mL⁻¹ penicillin, and 4 mM of L-glutamine. The cells were cultivated at 37 °C in a humidified 5 % CO₂ atmosphere. The uncured monomer resins were tested in a concentration range from 0 to 5 mM (UDMA and VCPMe₃hexAmid). This concentration range corresponds to up to 2 vol.% DMSO per well, i.e., a concentration already slightly toxic for the cells. The VCPHexEster resin was tested at concentrations up to 20 mM corresponding to up to 8.9 vol.% DMSO per well, i.e., a concentration highly toxic for the cells (Fig. S15). The cells were seeded at a density of 1 x 10⁴ cells per well, in 96-well plate, 24 h prior to the experiment. As 100 % viability control, untreated cells were used. For each dilution step, eight replicates were used. After dissolving the metabolically formed formazan crystals in isopropanol, the absorbance was measured using a plate reader (Genios Pro, Tecan) at a wavelength of 580 nm. For data evaluation the software

SigmaPlot 11.0 from the Systat Software GmbH was used, the x-scale was plotted logarithmically, and a nonlinear fit was run to obtain the lethal dose 50 (LD₅₀) values. Group data are reported as mean \pm standard deviation. Statistical significance was defined as having $p < 0.001$.

Monomer Synthesis

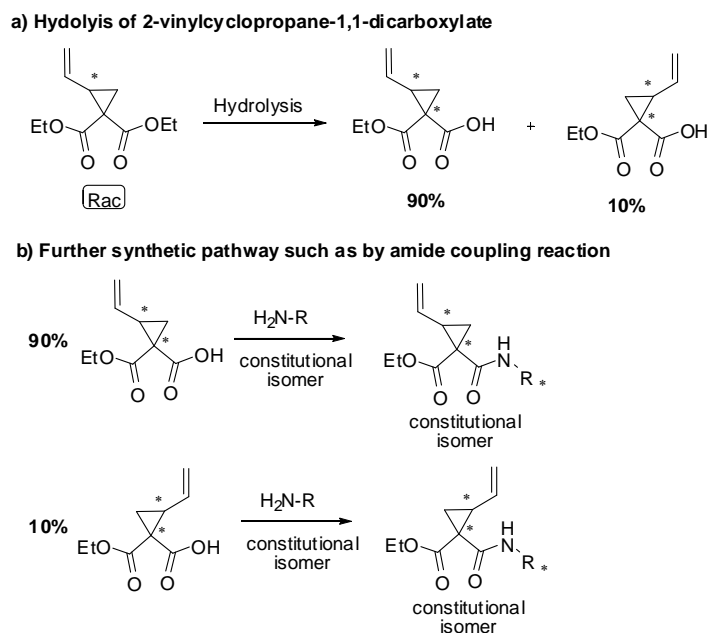
Synthesis of diethyl 2-vinylcyclopropane-1,1-dicarboxylate (1) and 1-(ethoxycarbonyl)-2-vinylcyclopropanecarboxylic acid (1a)

Diethyl 2-vinylcyclopropane-1,1-dicarboxylate was obtained as mono-functional VCP, using diethyl malonate and the corresponding dibromo butane as per published procedure.^[2,3] The chemical hydrolysis of 1 to the 1-(ethoxycarbonyl)-2-vinylcyclopropanecarboxylic acid was obtained with 1.10 eq. of potassium hydroxide as per published procedure.^[4]

Complexness of isomerization for VCP derivatives

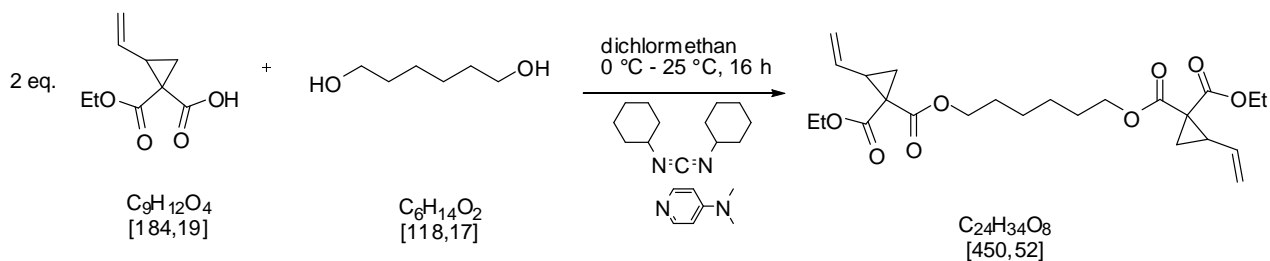
The hydrolysis of the racemic 2-vinylcyclopropane-1,1-dicarboxylate (1) results in a racemic mixture of diastereoisomers in a ratio of about 90:10.^[4] With continuing process of synthesis, and using isomeric spacer elements like for VCPMe₃hexAmid, the isomeric complexity increase further. Therefore, to avoid losing a general overview over the basic monomer structure, only the most probable isomeric structure was presented within the main part of the manuscript and following figures and schemes. An exemplary structural description of a VCP derivative is presented in Scheme S1.

Scheme S1. Exemplary structural description of the stereo centers and the isomerization complexity of VCP derivatives.



Synthesis of 1,2-bis[(1-ethoxycarbonyl-2-vinylcyclopropan-1-yl)carbonyloxy]hexane (VCPhexEster)

Scheme S2. Synthesis of bi-functional vinylcyclopropane ester (VCPhexEster).



A flame-dried and with argon purged flask was charged with 200 mL of anhydrous DCM. 24.18 g (1.20 eq., 0.117 mol) of DCC were introduced and dissolved by stirring. This solution was transferred to a flame-dried funnel, which was connected to a flame dried 500 mL three-necked reaction flask. This three-necked reaction flask was charged with 100 mL of anhydrous DCM, 21.59 g (1.20 eq., 0.117 mol) of 1a, 0.596 g (0.05 eq., 4.9×10^{-3} mol) of DMAP and 5.771 g (0.50 eq., 0.049 mol) of anhydrous 1,6-hexanediol and stirred for 15 min at room temperature. Subsequently, the reaction solution was cooled to 0 °C and the DCC solution with a drip rate of about 60 mL h⁻¹ was added drop wise. The reaction solution was stirred for 16 h at room

temperature. Subsequently the reaction mixture was filtered through a Büchner funnel, thereby resulting urea derivatives have been filtered off. The pale yellow solution was washed with 1 molar NaOH solution (1 x 100 mL), 1 molar HCl solution (1 x 100 mL) and with neutral water (3 x 50 mL). After drying over anhydrous magnesium sulfate, the solution was deposited on 32 g silica gel and purified by flash chromatography (medium pressure liquid chromatography MPLC-system), using hexane and ethyl acetate as eluent. The purified phase of 1,2-bis[(1-ethoxycarbonyl-2-vinylcyclopropan-1-yl)carbonyloxy]hexane (VCP_{hex}Ester) was annexed with 150 ppm BHT and dried in vacuo; yield: 75 %, colorless liquid. ¹H-NMR (300 MHz, CDCl₃): δ = 5.47-5.35 (m, 2 H, CH=CH₂), 5.30-5.27 (m, 2 H, CH=CHH), 5.14-5.10 (m, 2 H, CH=CHH), 4.23-4.02 (m, 8 H, O-CH₂), 2.59-2.51 (m, 2 H, CH-CH), 1.72-1.60 (dd, ³J_{HH} = 9.0, ²J_{HH} 4.9 Hz, 2 H, CHH-CH; m, 4 H, -CH₂-), 1.55-1.50 (dd, ³J_{HH} = 9.0, ²J_{HH} = 4.9 Hz, 2 H, CHH-CH), 1.40-1.31 (m, 4 H, CH₂-CH₂), 1.24 (t, ³J_{HH} = 7.1, 6 H, CH₃); ¹³C-NMR (75 MHz, CDCl₃) δ = 169.8 (O-C=O), 167.4 (O-C=O), 133.2 (CH=CH₂), 118.6 (CH=CHH), 65.6 (O-CH₂), 61.6 (O-CH₂), 36.0 (C4), 31.3 (-CHH), 28.5 (-CH₂), 25.6 (-CH₂), 20.5 (CH-CH), 14.3 (-CH₃); FT-IR (attenuated total reflectance (ATR)): ν = 3085 (w), 2980 (w), 2938 (w), 2862 (w), 1722 (s), 1639 (w), 1465 (w), 1443 (w), 1370 (m), 1317 (m), 1266 (s), 1195 (s), 1129 (s), 1032 (m), 990 (w), 958 (w), 915 (m), 862 (w), 778 (w), 748 (w), 707 (w), 665 cm⁻¹ (w).

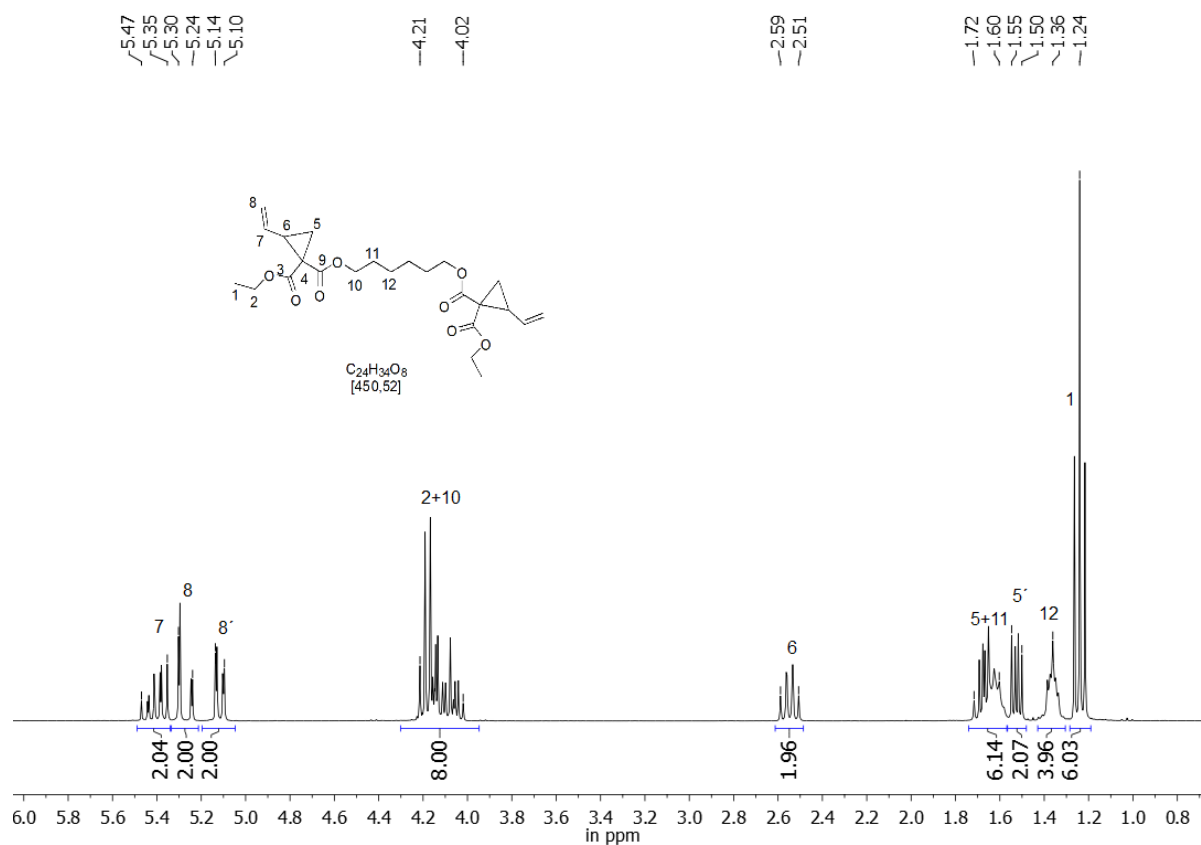


Figure S1. ¹H NMR of VCPHexEster (CDCl₃, 300 MHz).

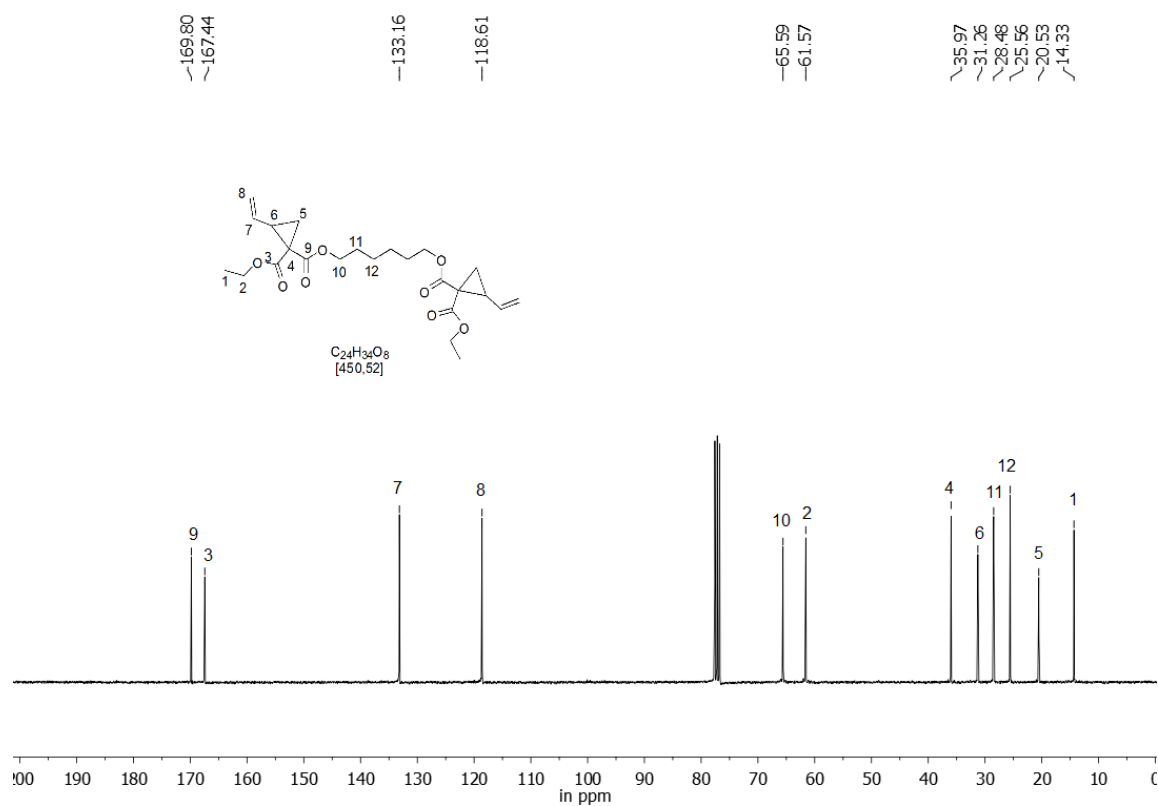


Figure S2. ¹³C NMR of VCPHexEster (CDCl₃, 75 MHz).

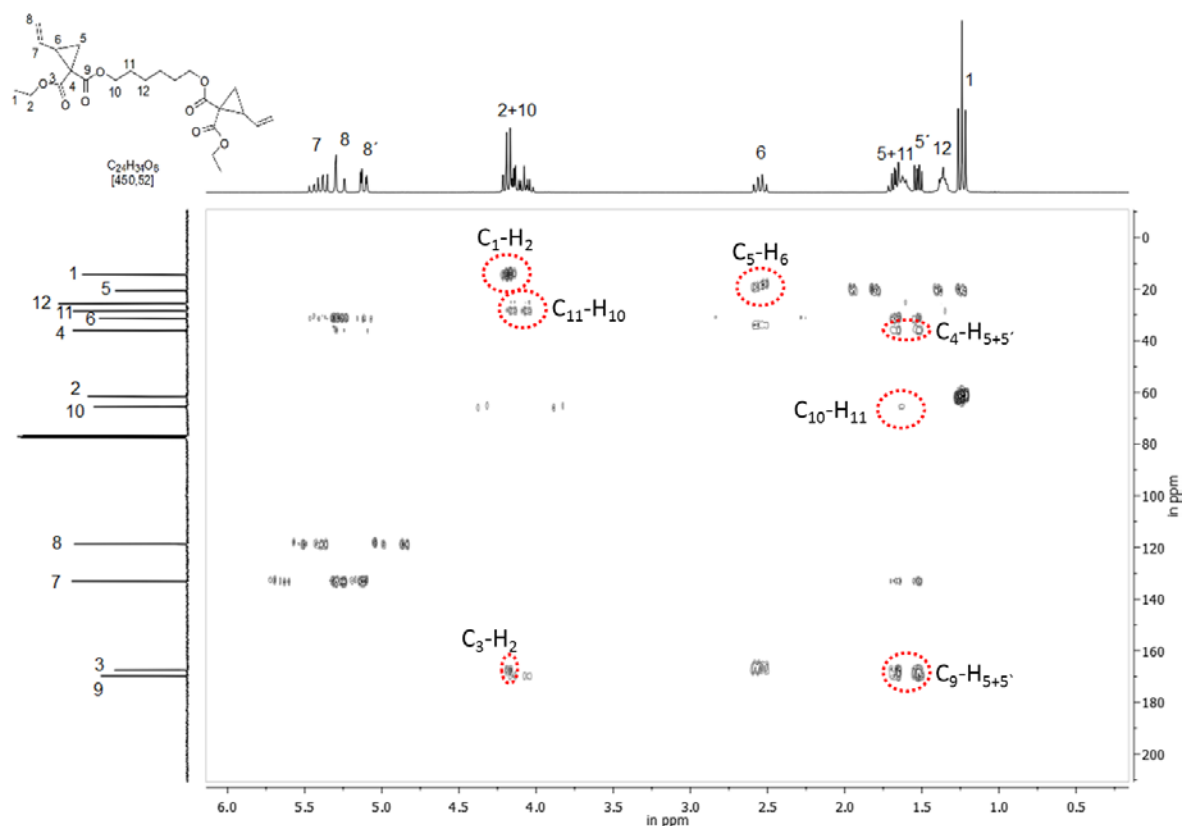


Figure S3. 2D-HMBC NMR of VCPHexEster (CDCl_3 , 300 MHz).

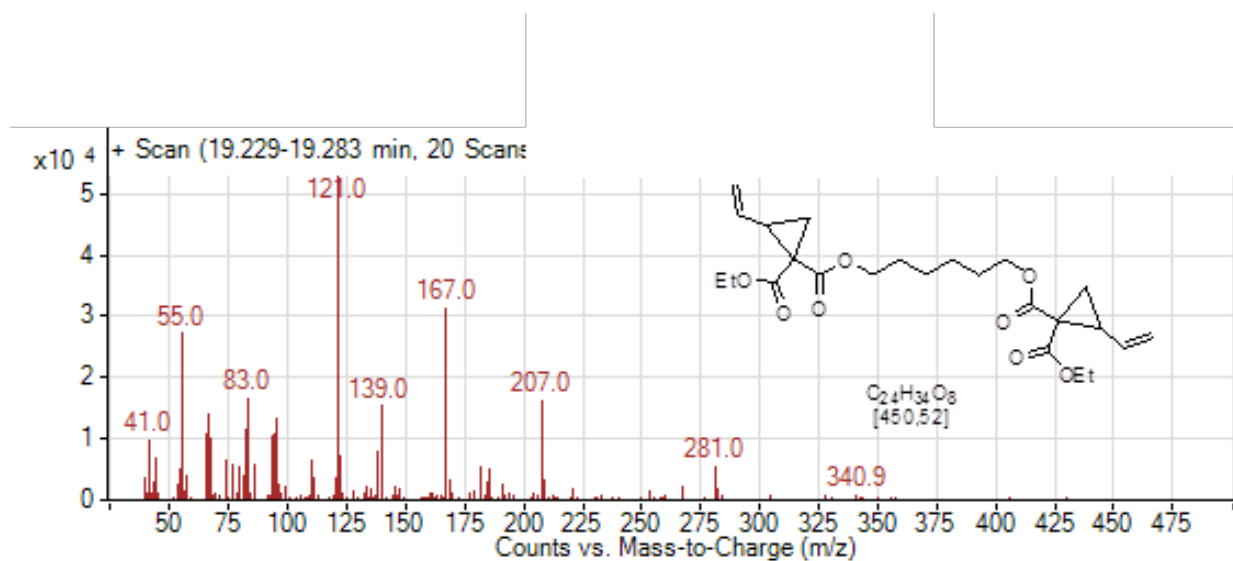
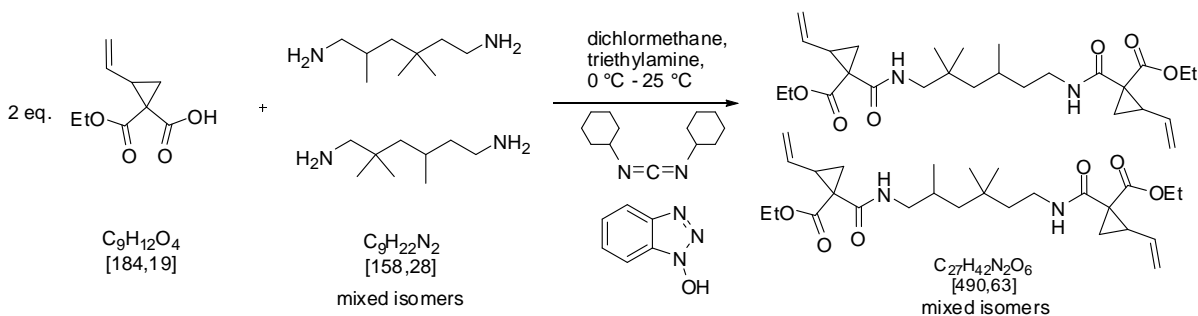


Figure S4. Mass spectra (Quadropol MS Agilent 5977A MSD: EI with 1000 eV) of GC-MS detected VCPHexEster. The VCPHexEster mass peak with ~ 450 m/z is due the low intensity and the fragmentation within this image section not visible.

Synthesis of diethyl-1,1'-(2,4,4-trimethylhexane-1,6-diyl)bis(azanediyl)bis-(oxomethylene)bis(2-vinylcyclopropanecarboxylate) (VCPMe₃hexAmid)

Scheme S3: Synthesis of bi-functional vinylcyclopropane amide (VCPMe₃hexAmid).



A flame-dried and with argon purged flask was charged with 15.28 g (0.50 eq., 0.051 mol) of 2,2,4,4-trimethyl-1,6-hexandiamine and diluted with 200 mL of anhydrous DCM. This solution was transferred to a flame-dried funnel, which was connected to a flame dried 1000 mL three-necked reaction flask. This three-necked reaction flask was charged with 200 mL of anhydrous DCM, 20.65 g (1.10 eq., 0.112 mol) of 1a, 23.13 g (1.1 eq., 0.112 mol) of DCC and stirred for 15 min at room temperature, then cooled to 0 °C and charged with 29.66 mL (2.1 eq., 0.214 mol) of triethylamine. Subsequently, the diamine solution with a drip rate of about 40 mL h⁻¹ was added drop wise. The reaction solution was stirred for 16 h at room temperature. Subsequently the reaction mixture was filtered through suction filter. The pale yellow solution was washed with water (2 x 100 mL), 1 molar HCl solution (1 x 100 mL) and with neutral water (3 x 50 mL). After drying over anhydrous magnesium sulfate, the solution was deposited on 35 g silica gel and purified by flash chromatography (MPLC-system), using hexane and ethyl acetate as eluent. The purified phase of diethyl-1,1'-(2,4,4-trimethylhexane-1,6-diyl)bis(azanediyl)bis-(oxomethylene)bis(2-vinylcyclopropane-carboxylate) (VCPMe₃hexAmid) was annexed with 800 ppm BHT and dried in vacuo; yield: 81 %, colorless liquid. ¹H-NMR (300 MHz, CDCl₃): δ = 8.49-8.09 (m, 2 H, NH), 5.74-5.52 (m, 2 H, CH=CH₂), 5.28-5.18 (m, 2 H, CH=CHH), 5.09-5.02 (m, 2 H, CH=CHH), 4.21-4.00 (m, 4 H, O-CH₂), 3.30-2.89 (m, 4 H, NH-CH₂), 2.49-2.27 (m, 2H, CH-CH), 2.01-1.93 (m, 2H, -CHH), 1.80-1.75 (m, 2H, -CHH), 1.73-1.65 (m, -CH) 1.56-1.30 (m, -CH; m, -CH₂), 1.24-1.16 (m, CH₃; -CH₂), 1.01 (m, -CH₂, CH), 0.92-0.88 (m, 3H, -CH₃), 0.86 (s, 6H, -CH₃); ¹³C-NMR (75 MHz, CDCl₃) δ = 171.6-171.5 (NH-C=O), 168.1-167.8 (NH-C=O), 133.5 (CH=CH₂), 119.6 (CH=CHH), 61.6-61.5 (O-CH₂), 47.7-47.6 (NH-CH₂), 47.0 - 46.8

(CH₂), 42.0, 41.9-38.2 (-CH₂), 37.1-36.3 (CH-CH), 35.0-34.4 (C₄), 33.20-25.5 (-CH₃), 29.2+29.1 (C₄), 21.4-21.0 (-CHH), 14.3 (-CH₃); FT-IR (attenuated total reflectance (ATR)): ν = 3360 (m, broad), 3085 (w), 2960 (m), 2933 (m), 2872 (w), 1705 (s), 1654 (s), 1533 (s), 1469 (m), 1446 (m), 1392 (w), 1371 (m), 1337 (w), 1314 (s), 1265 (m), 1198 (m), 1140 (s), 1020 (m), 992 (m), 960 (w), 914 (m), 865 (m), 835 (w), 773 (w), 740 cm⁻¹ (w).

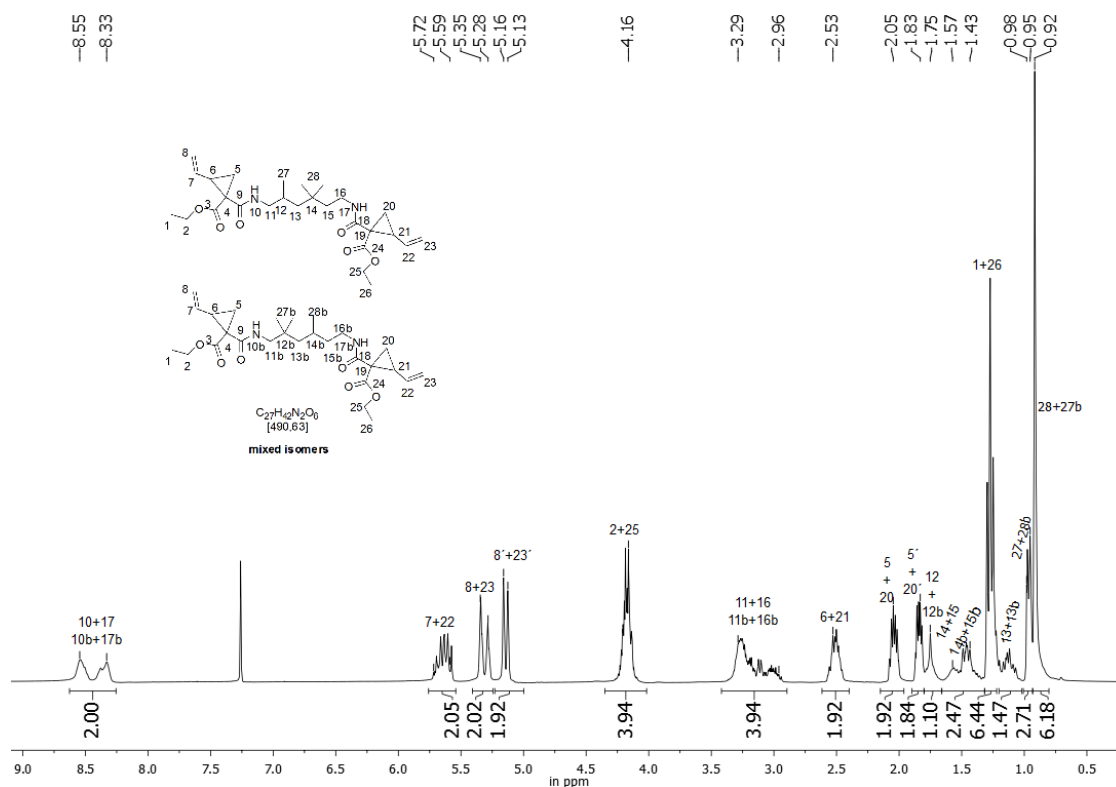


Figure S5. ¹H NMR of VCPMe₃hexAmid (CDCl₃, 300 MHz).

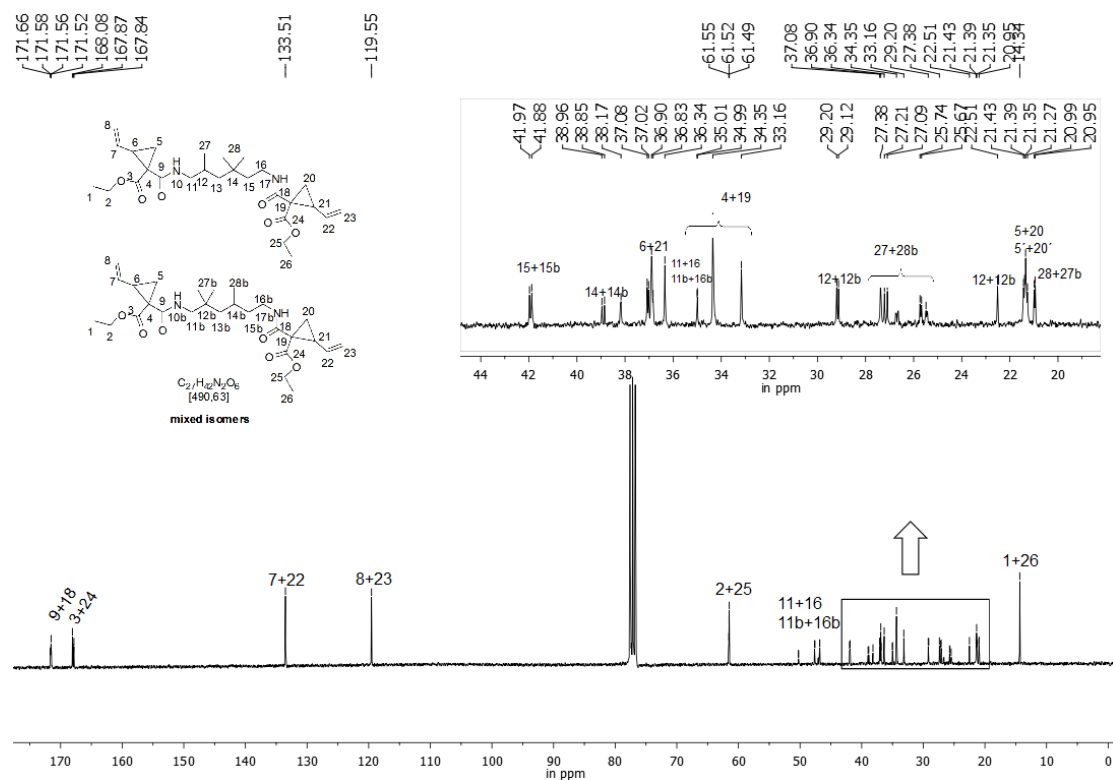


Figure S6. ^{13}C NMR of VCPMe₃hexAmid (CDCl_3 , 75 MHz), inclusive an expansion from ^{13}C NMR between 45-18 ppm.

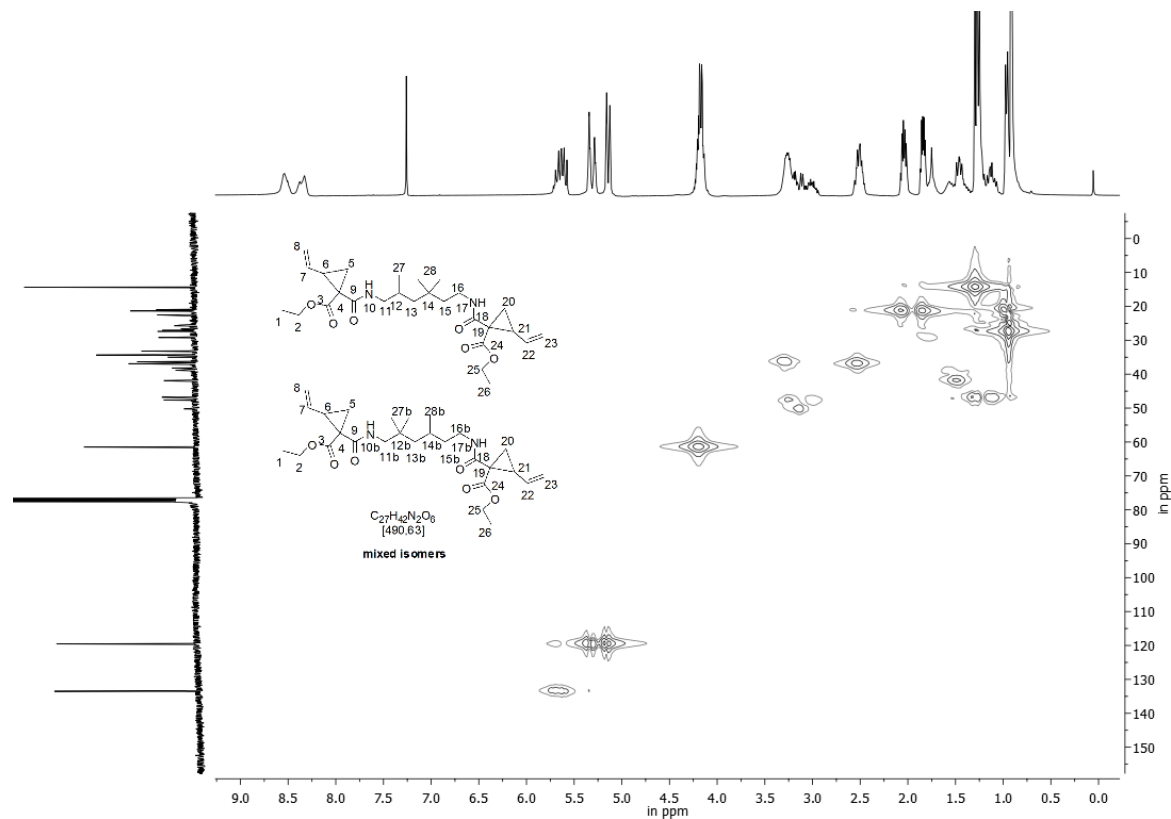


Figure S7. 2D-HSQC NMR of VCPMe₃hexAmid (CDCl_3 , 300 MHz).

Supplementary Analytical Data

Temperature variable ^1H -NMR experiment to confirm the hydrogen bonding effect of the VCP-amide resin (VCPMe₃hexAmid)

The temperature dependence of the amide protons or rather their chemical shift with temperature is well known in the literature.^[5] The main reason of this effect is associated to the presence of H-bonds.^[6] Generally, at higher temperature amide protons become shifted to the high field (Figure S8), as with increased temperatures a decreased deshielding effect is anticipated. For non-hydrogen bonded protons firstly the effect of temperature is generally weaker, and on the other hand often inversely proportional, as these protons become slightly shifted to the low field. Within the identical temperature range of the ^1H -NMR experiment for the corresponding VCP-ester derivative (VCPhexEster) no similar characteristic hydrogen-bonding shifts could be observed. Only the weaker and common temperature effect of the non-hydrogen bonded protons could be monitored. A graphical plot of the chemical shift during the variable ^1H -NMR temperature experiments is provided within Figure S9.

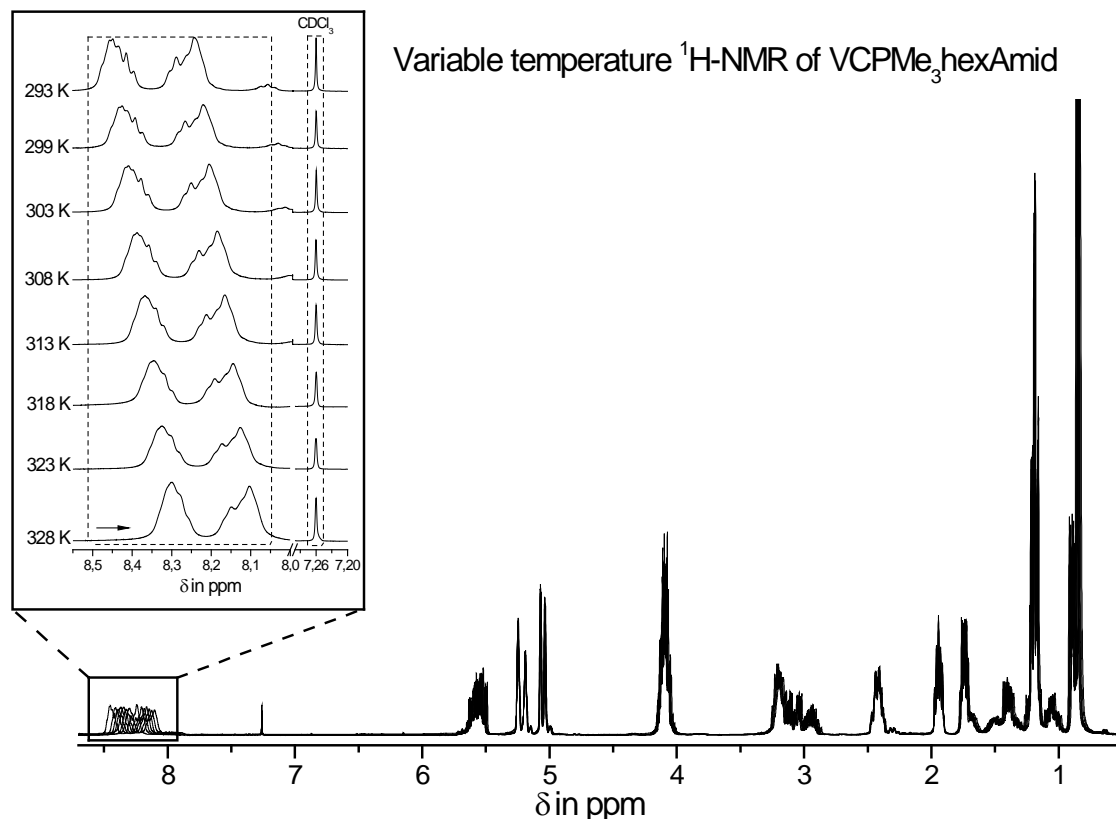


Figure S8: Variable temperature ^1H -NMR of VCPMe₃hexAmid (0.5 mM in CDCl_3 , 300 MHz) between a temperature range of 293 – 328K. The temperature dependence of the amide protons indicates the presence of intermolecular hydrogen bonding effects. All spectra were calibrated to the CDCl_3 signal at 7.26 ppm.

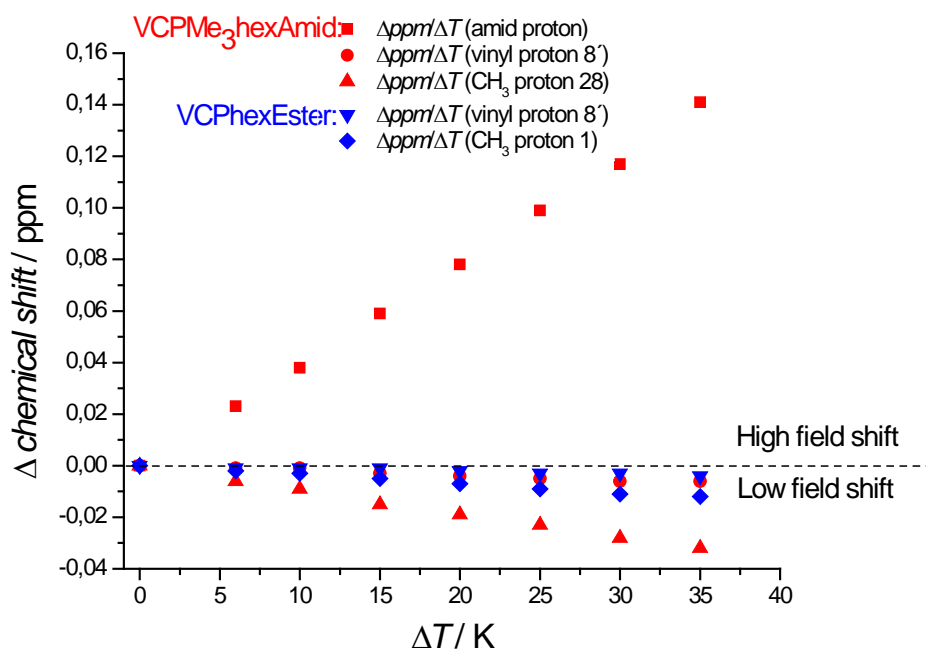
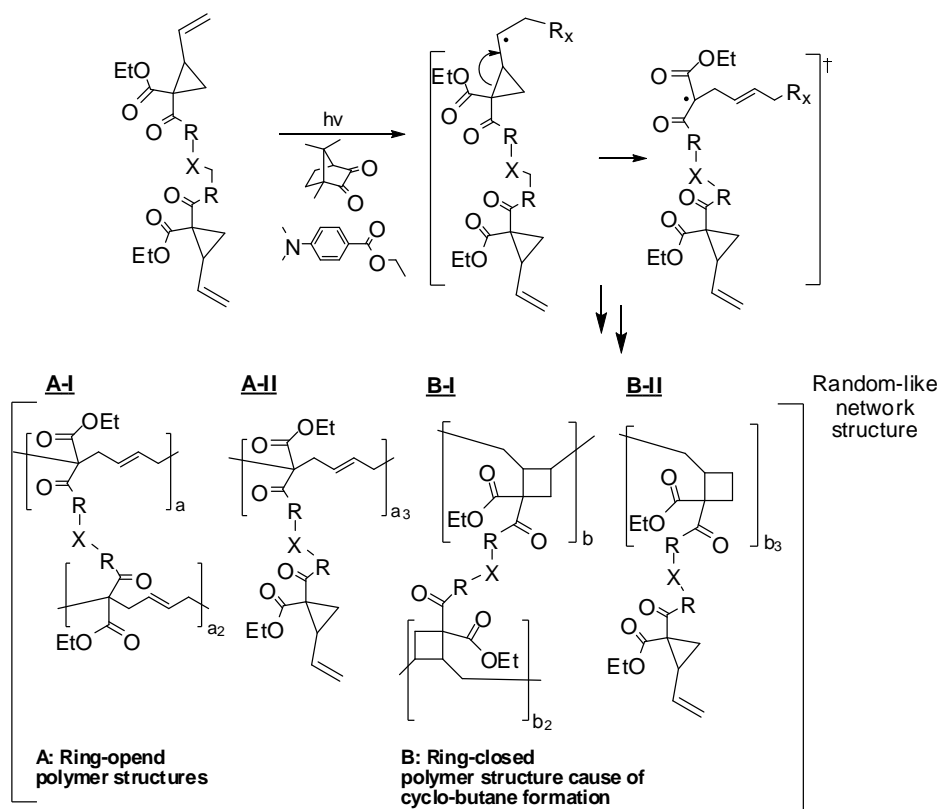


Figure S9: Graphical plot of the some selected proton shifts during variable ^1H -NMR temperature experiments. Only the amide proton signal of the VCPMe₃hexAmid shows a characteristic shift to higher magnetic fields, which proved the presence of hydrogen bonding for this monomer.

Photo-polymerization mechanism of bi-functional VCP derivatives

The radical photo-polymerization of substituted VCPs results mainly in 1,5-ring-opened polymers units,^[3] however, the competitive cyclization reaction predominately to cyclobutane containing units can minimize the benefit of the ring cleavage.^[2,3] Therefore several independent polymer units for the cross-linking of VCPs are likely (Scheme S4). The relation of these units depends upon polymerization temperature, viscosity and conversion.^[3] So far an unambiguous structural elucidation of cured VCP networks is by the current spectroscopic state of the art techniques difficult, as no technique can resolute and quantify clearly between the cyclobutane-units (B-I and B-II) and the ring-opened units (A-I and A-II) as shown in Scheme S4. Nevertheless, residual monomer because of incomplete conversion can be quantified with extraction experiments (included in the main part of the manuscript). Further, the concentration of partially polymerized VCP units (A-II) seemed to be very low for VCPMe₃hexAmid as described in the main part of the manuscript, based on the results of the solid state NMR.

Scheme S4. Schematic radical induced photo polymerization mechanism of bi-functional VCP derivatives.



High resolution solid state ^{13}C -NMR spectroscopy of cured VCPMe₃hexAmid

High-resolution solid state ^{13}C -CP/MAS (cross polarization/magic angle spinning) NMR Spectra of cured VCPMe₃hexAmid were measured by a Bruker spectrometer operating at 100.6 MHz. Within the ^{13}C -CP/MAS spectrum of the cured VCPMe₃hexAmid (directly after curing) the peak at 119.7 ppm defines clearly the vinyl-carbon atom 8 + 23 of the VCPMe₃hexAmid (Figure S6). In contrast the peak at 129.3 ppm defines the carbon signal of the C=C double bond of the ring-opened VCP-unit.^[3] After extraction of residual monomer the peak at 119.7 ppm has gone, only a light shoulder remained, indicating an incomplete but extraordinary high cross-linking (dedicated to the structures of A-II and B-II of Scheme S4). Unfortunately an explicit quantification was not possible as the signal intensity was outside the current detection limit for this method. Further, as mentioned in the main part of the manuscript the formation of cyclobutane-units should be taken into consideration also. As mentioned above an unambiguous structural elucidation of cured VCP networks is unfortunately by the current state of the art techniques difficult, as no technique can resolve clearly between the cyclobutane-units and the ring-opened units as shown in Scheme S4.

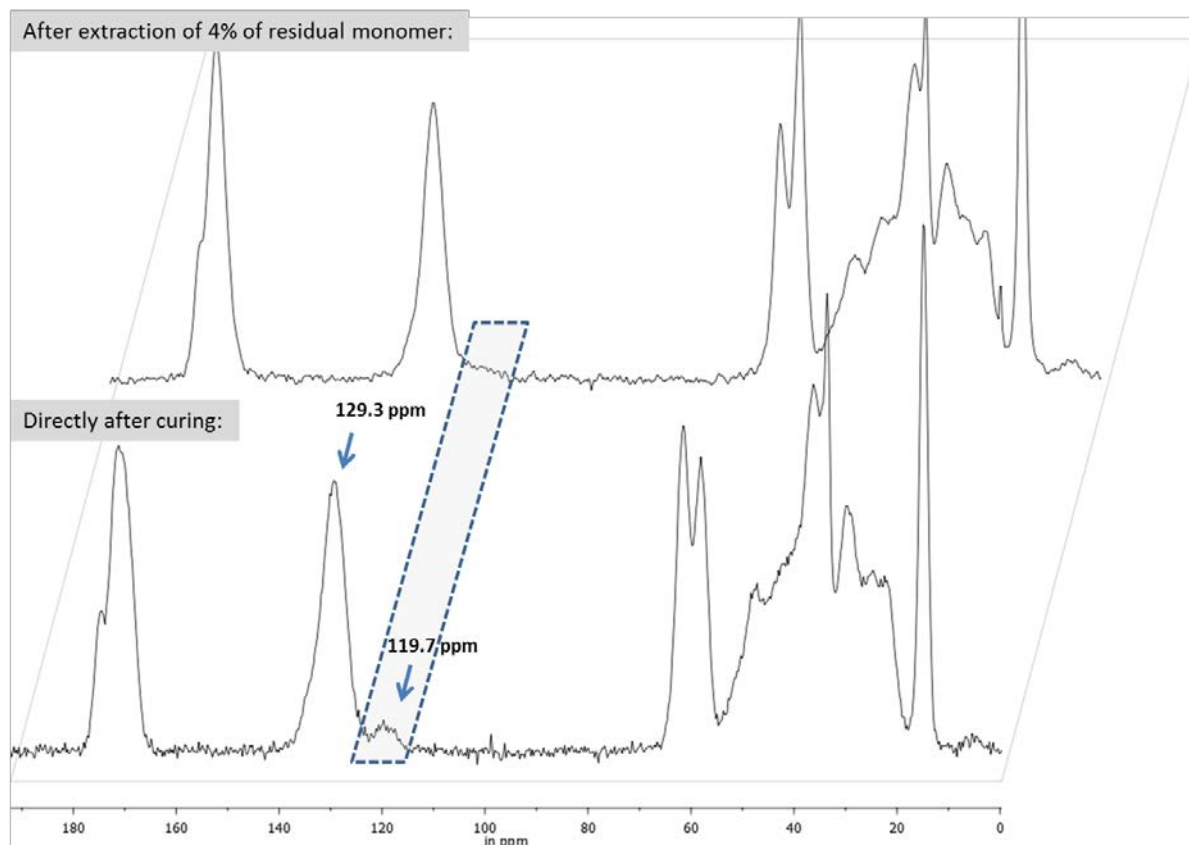


Figure S10: ^{13}C -CP/MAS NMR spectra (100MHz) of cured VCPMe₃hexAmid. The lower spectrum shows a cured VCPMe₃hexAmid sample directly after curing. The upper graph shows the analogue sample after extraction of 4% of residual monomer. The peak at 129.3 ppm defines the carbon signal of the C=C double bond of the ring-opened VCP-unit. The peak at 119.7 ppm defines clearly the vinyl-carbon atom 8+23 of the VCPMe₃hexAmid (Figure S6).

Spectroscopic Ellipsometry: Refractive index measurements

Illustration of the wavelength-dependent dispersion of the refractive index. The refractive index at 589 nm was calculated by averaging over the five values of each sample at 589 nm.

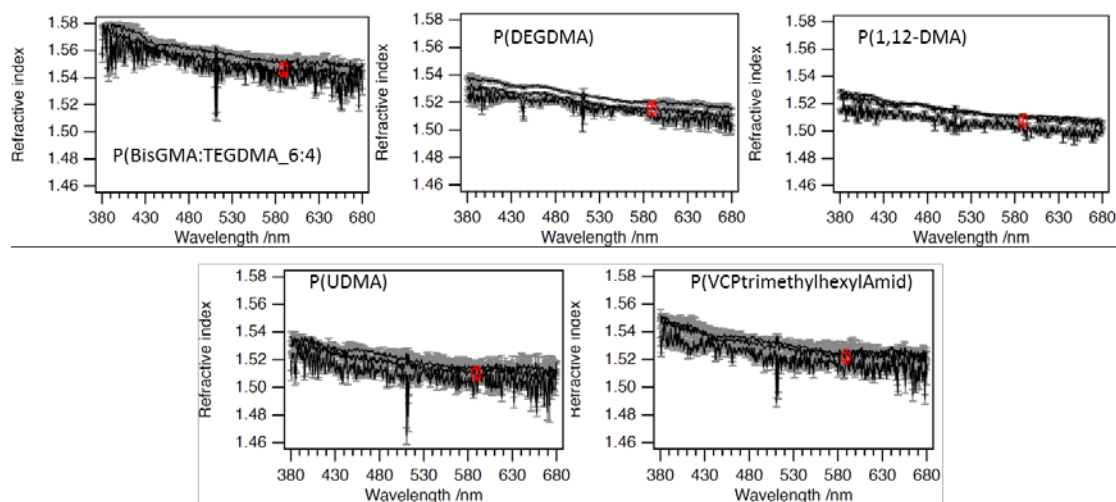


Figure S11. Within SE-determined refractive indices. The graphic display shows the refractive index in dependence of the wavelength. The average value of each specimen at 589 nm has been used for evaluation within the main part

of the manuscript.

Determination of mechanical properties (E-Modulus)

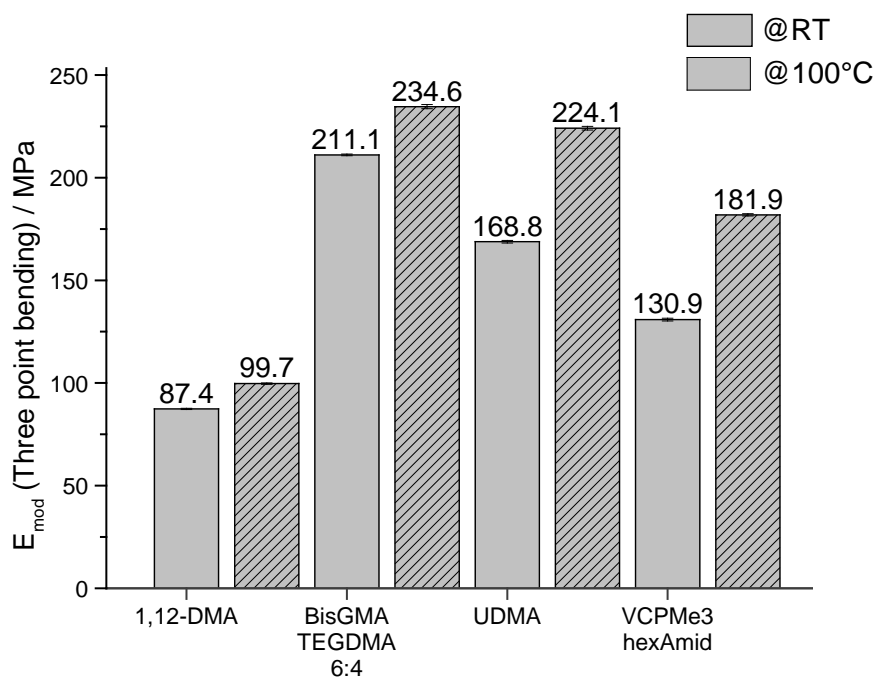


Figure S12. E-modules values of three point bending experiments for cured specimens with sizes of 25x3x1 mm³. The examinations of the specimens have been carried out once directly after curing and secondly after 12 h storage at 100 °C in vacuo to determine additionally the potential modulus after partial relaxation of internal network tensions.

Determination of residual monomer amount of cross-linked samples by extraction experiments

GC calibration for VCPhexEster:

The GC measurements have been done by a GC-FID system as described within the experimental section for methods. The calibration ranged between ~7 mg mL⁻¹ up to 14 µg mL⁻¹ (Figure S13).

GC calibration for VCPHexylEster

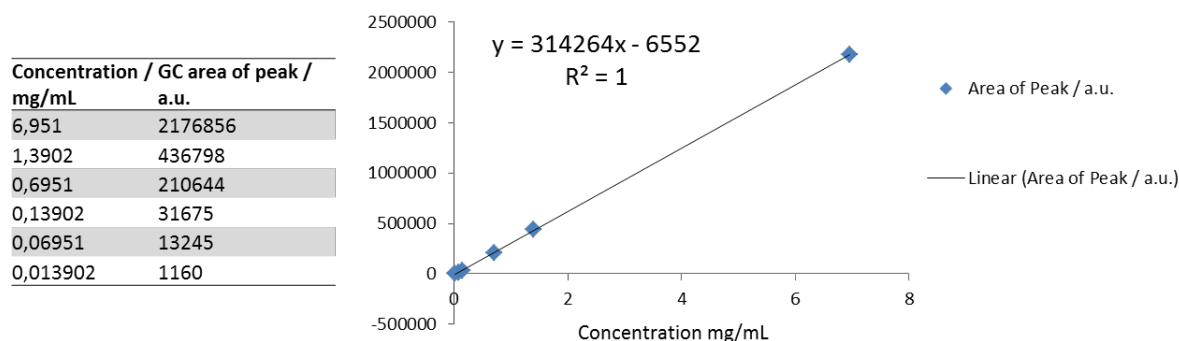


Figure S13. GC calibration for VCPHexEster in a range between $\sim 7 \text{ mg mL}^{-1}$ up to $14 \text{ } \mu\text{g mL}^{-1}$.

NMR calibration for VCPMe₃hexAmid:

For VCPMe₃hexAmid no GC measurements could be performed, as this monomer cannot enter into the gas phase due its higher molar mass and polarity. Therefore, a NMR calibration of VCPMe₃hexAmid has been carried out. By comparison the integration areas of the respective ¹H-NMR proton signals (amide-, vinyl and cyclopropane-protons) to the proton signals of mesitylene, which has been added to the CDCl₃ as internal standard in $2.8216 \text{ mg mL}^{-1}$ amount. The concentration range of the established calibration curve of the VCPMe₃hexAmid amounted between 5 mg mL^{-1} up to $10 \text{ } \mu\text{g mL}^{-1}$. For each ¹H-NMR a number of scans of 2048 has been chosen to achieve an appropriate signal to noise resolution.

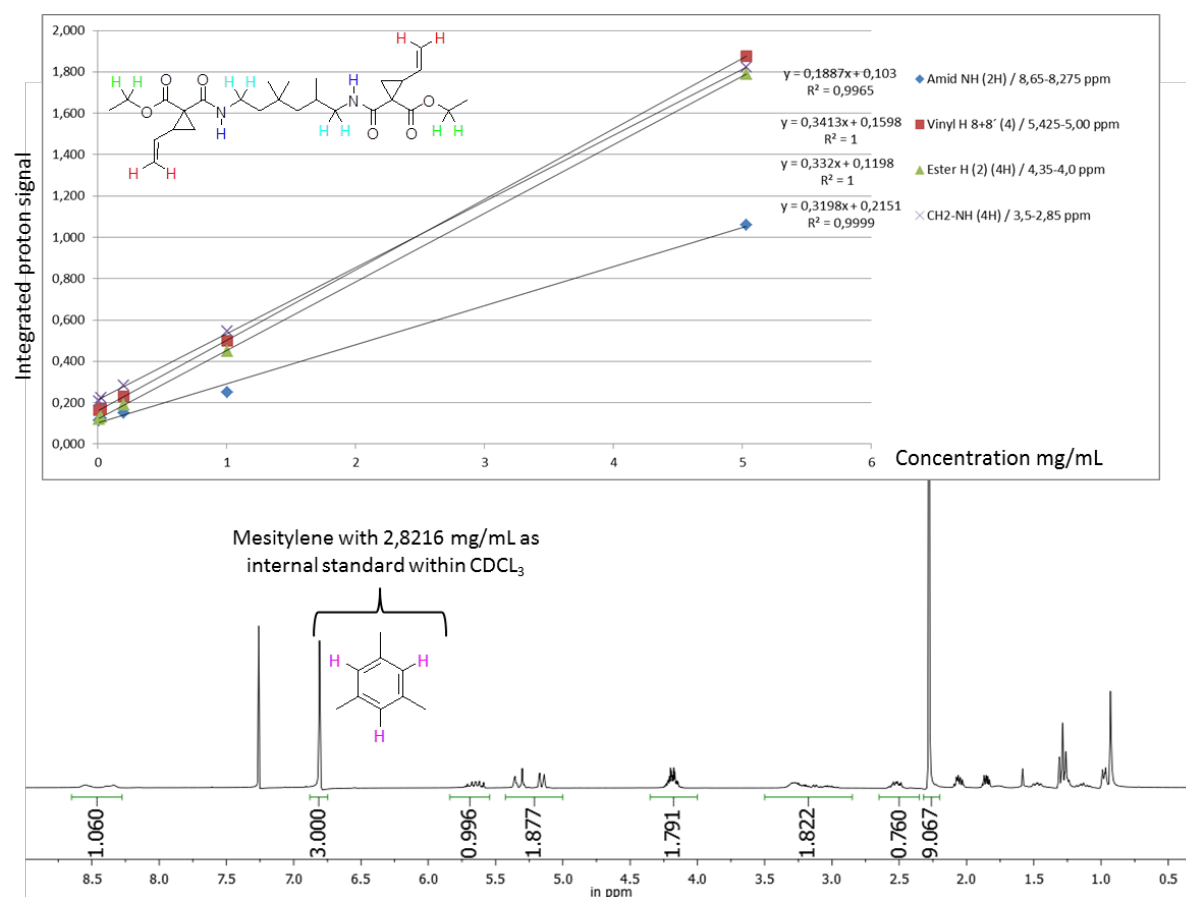


Figure S14. ^1H -NMR calibration of VCPMe₃hexAmid, inclusive an exemplary proton NMR of a sample with a concentration of 5.03 mg mL⁻¹.

With these calibration curves, the residual monomer amount was determined by extraction experiments. For VCP_{hex}Ester the cured and weighted samples have been immediately immersed after radiation to 5.0 mL of chloroform (as extraction fluid) in 10 mL bottles with snap-on caps for 24 h respectively. The bottles have been shaken slightly within a Heidolph Multi Reax shaking system (~500 rpm). Afterwards the supernatant solution has been directly transferred, without any further process, to a GC vial to be measured. Analog to VCPMe₃hexAmid, the weighted and samples have been immediately immersed after radiation to the CDCl₃ solution (inclusive the mesitylene standard) for 24 h, respectively. Analog to VCP_{hex}Ester the bottles have been shaken slightly within a Heidolph Multi Reax shaking system (~500 rpm). Afterwards 0.7 mL of the supernatant solution has been directly transferred to a NMR vial to be measured.

Compilation of characteristic resin features

Within the main part of the manuscript, several resin features have been mentioned without further specifications. In order to classify all mentioned resins in detail by numerical values within Table S1 relevant data was summarized.

Table S1. Compilation of relevant resin properties, registered with their numerical values.

	1,12-DMA	UDMA	BisGMA	BisGMA- TEGDMA_ 6:4	VCPhex Ester	VCPMe ₃ hex Amid
Molecular weight / g mol ⁻¹	338.48	470.56	512.59	422.08	450.52	490.63
Viscosity ^{a)} / Pa s	<0.01	13.8	~1400 ^[7]	0.61	0.08	2.38
Volume shrinkage ^{b)} / %	11.1	8.9	4.7 ^[8]	5.9	-	4.9
E _{mod} ^{c)} / MPa	87.4	168.8	-	211.1	-	130.9
Refractive index ^{d)} (uncured) @589 nm	1.461	1.485	1.549 ^[9]	1.512	1.478	1.499
Refractive index ^{e)} (cured) @589 nm	1.511	1.508	-	1.547	-	1.522
Vickers hardness ^{f)}	0.81	1.80	-	2.18	-	1.55
LD ₅₀ ^{g)} / mM	>5.00 ^[10]	0.071 ± 0.009	0.08 ± 0.03 ^[8]	-	6.3 ± 2.3	0.067 ± 0.005

^{a)} Determined at 25 ± 0.5 °C with shearing rate of 100 s⁻¹; ^{b)} determined by the Archimedes's principle; ^{c)} for specimens of the dimension 25x3x1 mm³, respectively; ^{d)} n_D²⁰ value determined by Abbe refractometer; ^{e)} determined by SE; ^{f)} average value of five specimens for measuring forces between 20, 40, 80, 120 and 200 mN; ^{g)} according to the norm ISO 10993-5.

Determination of Cytotoxicity:

The influence of VCPMe₃hexAmid and VCPhexEster resins on the metabolic activity of mammalian cells was tested by MTT assay and compared with UDMA used as reference. Therefore, the L929 cells were exposed to UDMA, VCPMe₃hexAmid and VCPhexEster for 24h.

The addition of the resins in the concentration range 0 to 20 mM affects the cellular metabolic activity in a concentration-dependent manner (Figure S15 and S16). Under these conditions, the LD₅₀ were 0.067 ± 0.005 mM and 6.3 ± 2.3 mM for cells treated with VCPMe₃hexAmid and VCPhexEster, respectively. For VCPhexEster, the cytotoxicities measured at concentrations ≥ 50 mM are similar to the ones detected with the solvent (i.e., DMSO) only (Fig. S16). Whereas, VCPMe₃hexAmid shows cytotoxicity comparable to UDMA (0.071 ± 0.009 mM), the VCPhexEster resin has an 88-fold higher LD₅₀ and is therefore less cytotoxic.

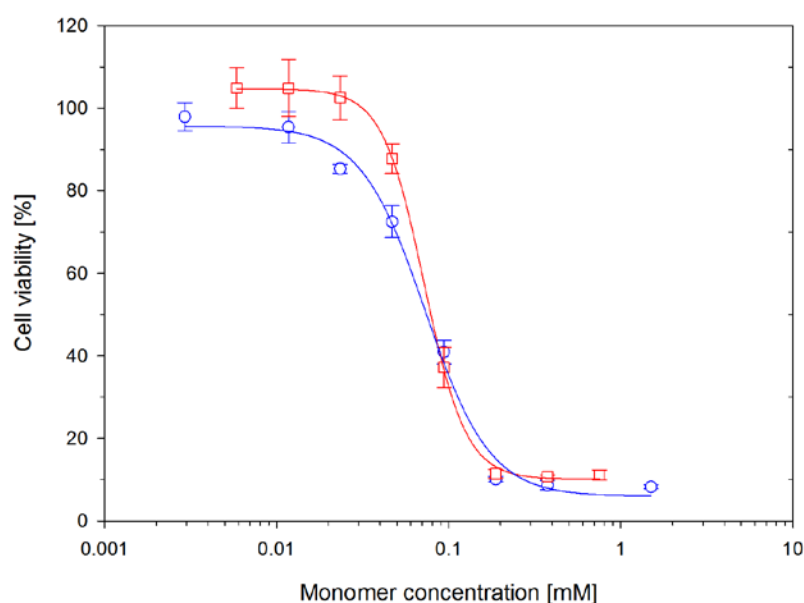


Figure S15. Cytotoxicity of the monomers in L929 cells. (a) Incubation period was 24 hours and cell seeding density 1×10^4 cells per well: (○) UDMA (used as a reference) and (□) VCPMe₃hexAmid. The data represent mean \pm standard deviation from three independent experiments. There is no significant difference between the curves ($p \leq 0.001$; t-test).

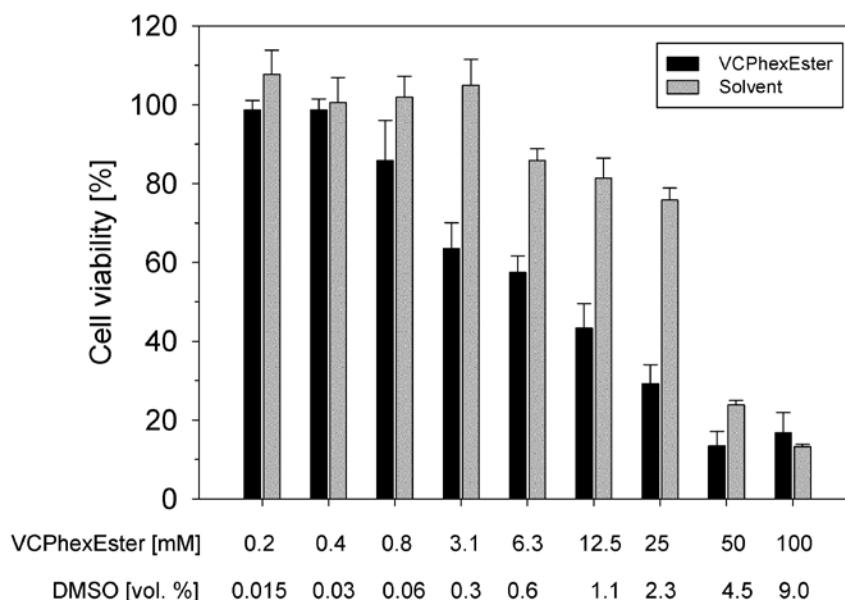


Figure S16. Cytotoxicity of the monomers in L929 cells. (a) Incubation period was 24 hours and cell seeding density 1×10^4 cells per well in 96-well plate. The data represent mean \pm standard deviation from three independent experiments.

References

- [1] T. W. H. Oates, H. Wormeester, H. Arwin, *Progress in Surface Science* **2011**, 86, 328–376.
- [2] F. Sanda, T. Takata, T. Endo, *Macromolecules* **1993**, 26, 1818–1824.
- [3] P. Pineda Contreras, P. Tyagi, S. Agarwal, *Polym. Chem.* **2015**, 6, 2297–2304.
- [4] a) V. Alupe, H. Ritter, *Macromol. Rapid Commun.* **2001**, 22, 1349–1353. b) N. Moszner, F. Zeuner, T. Völkel, U. K. Fischer, V. Rheinberger, *Journal of Applied Polymer Science* **1999**, 72, 1775–1782.
- [5] a) D.K. Kopple, M. Ohnishi, A. Go, *J. Am. Chem. Soc.*, **1969**, 91, 4264–4272. b) K. H. Scheit, *Angew. Chem.*, **1967**, 79, 190.
- [6] G. Wagner, A. Pardi, K. Wuthrich, *J. Am. Chem. Soc.*, **1983**, 105, 5948–5949.
- [7] S. G. Pereira, T. G. Nunes, S. Kalachandra, *Biomaterials* **2002**, 23, 3799–3806.
- [8] C.-M. Chung, J.-G. Kim, M.-S. Kim, K.-M. Kim, K.-N. Kim, *Dental Materials* **2002**, 18, 174–178.
- [9] C. A. Khatri, J. W. Stansbury, C. R. Schultheisz, J. M. Antonucci, *Dental Materials* **2003**, 19, 584–588.
- [10] W. Geurtsen, F. Lehmann, W. Spahl, G. Leyhausen, *J. Biomed. Mater. Res.* **1998**, 41, 474–480.